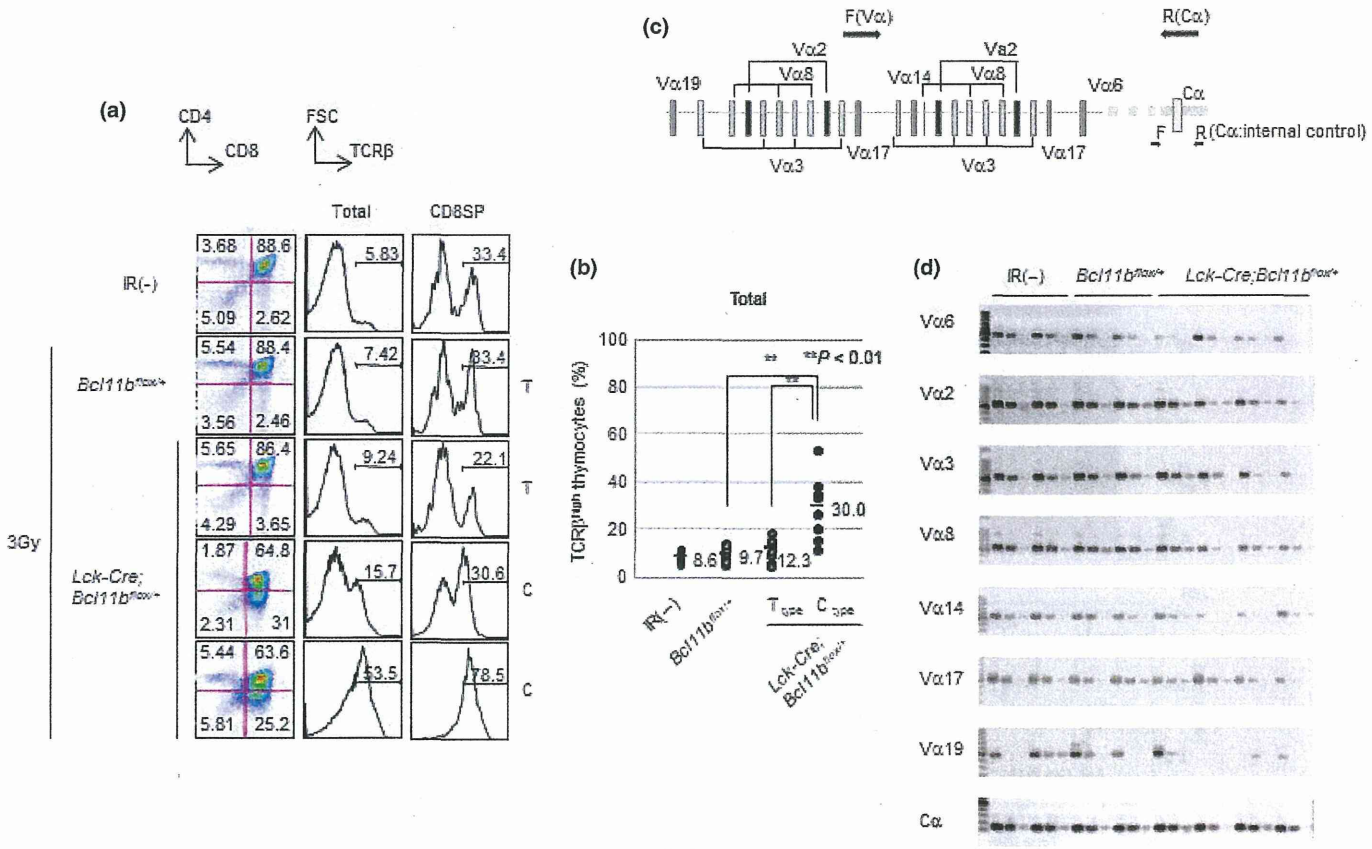

Fig. 2. Differentiation of thymocytes with clonal expansion (C-type) in irradiated *Bcl11b*$^{flox/+}$;*Lck-Cre* mice. (a) Left panels show flow cytometry of CD4 and CD8 expression in thymocytes. The middle and right panels show T-cell receptor-β (TCRβ) expression (horizontal axis) and cell number (vertical axis) in total thymocytes and in the CD8$^+$ fraction, respectively. CD8SP, CD8$^+$ single-positive thymocytes; IR(−), non-irradiated mice. (b) Percentage of TCRβ^{high} cells in non-irradiated, irradiated *Bcl11b*$^{flox/+}$ thymocytes, control (T-type), and C-type thymocytes. (c) Diagram shows part of the TCRα locus and the relative location of PCR primers used. (d) Panels show patterns of Vα-Cα rearrangement in non-irradiated and irradiated *Bcl11b*$^{flox/+}$ thymocytes, and T-type and C-type thymocytes. The cDNA obtained from thymocytes was diluted at three different concentrations and subjected to PCR using F primers of various Vα and unique Cα regions and a common R primer in the constant Cα region.

The number was significantly decreased in C-type thymuses and also T-type thymuses, but it was retained in irradiated *Bcl11b*$^{flox/+}$ mice at a similar level to that of non-irradiated mice. The result suggests impairment in the maintenance of thymocytes in *Bcl11b*$^{flox/+}$;*Lck-Cre* mice after γ-irradiation, as found in irradiated *Bcl11b*$^{KO/+}$ mice.[14] Figure 4(b) shows the number of thymocytes in irradiated *Bcl11b*$^{flox/+}$*CD4-Cre* mice. No decrease was observed.

Effect of loss of one *Bcl11b* allele on differentiation and cell cycle regulation. We examined differentiation of thymocytes in non-irradiated *Bcl11b*$^{flox/+}$ and *Bcl11b*$^{flox/+}$;*Lck-Cre* mice. Figure 5(a) shows representative flow cytometric analyses using CD4, CD8, and TCRβ, and Figure 5(b) summarizes the percentage of DN, ISP, DP, CD4SP, and CD8SP cells. The percentage of DN and ISP cells was increased in *Bcl11b*$^{flox/+}$;*Lck-Cre* mice relative to that of *Bcl11b*$^{flox/+}$ mice, whereas the percentage of DP, CD4SP, and CD8SP cells was decreased. This indicated that the *Lck-Cre*-induced loss of one *Bcl11b* allele provided two- or three-fold elevation in the percentage of immature thymocytes. Figure S4 shows flow cytometry analyses and the summary of the percentages of those cells in *Bcl11b*$^{flox/+}$;*CD4-Cre* mice. No significant change was observed.

We previously showed impairment of cell cycle arrest at the S phase in response to γ-irradiation in ISP cells of *Bcl11b*$^{KO/+}$ mice.[26] We thus examined the arrest in *Bcl11b*$^{flox/+}$ and *Bcl11b*$^{flox/+}$;*Lck-Cre* mice. To monitor the cell cycle, we injected BrdU 1 h before 1 Gy γ-irradiation, and analyzed thymocytes 4 h after irradiation. Figure 6(a) shows results of flow cytometric analysis. The BrdU incorporation is shown on the vertical axis and FSC values on the horizontal axis, an indication of cell size. The BrdU$^+$ FSC^{large} fraction represents BrdU-incorporated cells in S and G_2/M phases of the cell cycle, whereas the BrdU$^+$ FSC^{small} fraction represents G_1 cells that have passed S phase after BrdU incorporation. Figure 6(b) summarizes the percentage of cells in the BrdU$^+$ FSC^{large} and BrdU$^+$ FSC^{small} fractions in ISP cells. Both fractions showed higher percentages in *Bcl11b*$^{flox/+}$;*Lck-Cre* mice than in *Bcl11b*$^{flox/+}$ mice, indicating more cells in the S phase and in the G_1 cells that have passed S phase. The result suggests that the *Lck-Cre*-induced loss of one *Bcl11b* allele attenuates radiation-induced cell cycle arrest at the S phase in ISP cells.

Discussion

In this paper, we examined clonal expansion of thymocytes in *Bcl11b*$^{flox/+}$;*Lck-Cre* and *Bcl11b*$^{flox/+}$*CD4-Cre* mice after γ-irradiation at an early stage prior to the time of thymic lymphoma development. In those mice, loss of one *Bcl11b* allele occurs in thymocytes at the DN2/DN3 and DP developmental stages, respectively. We found clonally expanding or C-type thymocytes in a half of *Bcl11b*$^{flox/+}$;*Lck-Cre* thymuses but not in *Bcl11b*$^{flox/+}$*CD4-Cre* thymuses, suggesting the origin of

doi: 10.1111/cas.12193
© 2013 Japanese Cancer Association

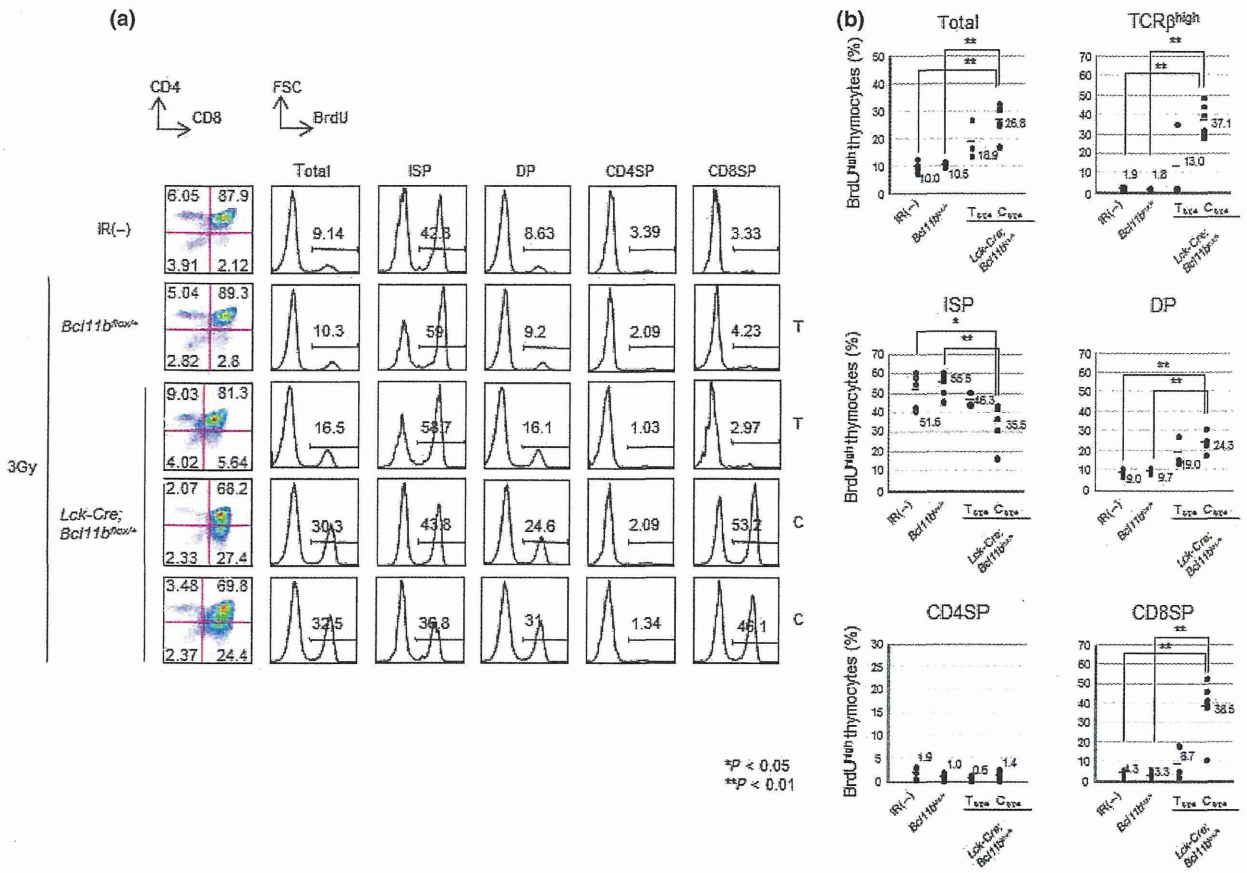

Fig. 3. Cell cycle regulation of C-type thymocytes in irradiated *Bcl11b*$^{flox/+}$;*Lck-Cre* mice. (a) Left panels show flow cytometric analysis of CD4 and CD8 expression, and the other panels show BrdU incorporation levels (horizontal axis) and cell number (vertical axis) in indicated subsets. The panels include results of thymocytes in non-irradiated (IR(–)) and irradiated *Bcl11b*$^{flox/+}$ mice as references. (b) Graphs show the percentage of BrdU^{high} thymocytes in indicated subsets of thymocytes. CD4SP, CD4$^+$ single-positive; CD8SP, CD8$^+$ single-positive; DP, double-positive; ISP, immature single-positive; TCRβ, T-cell receptor-β.

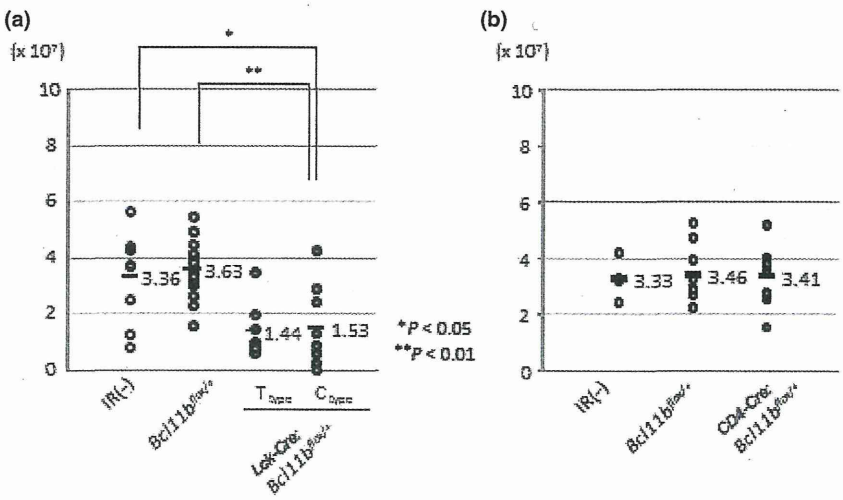

Fig. 4. Thymocyte number in *Bcl11b*$^{flox/+}$;*Lck-Cre* (a) and *Bcl11b*$^{flox/+}$;*CD4-Cre* (b) mice 60 days after irradiation. The graphs include cell number in non-irradiated and irradiated *Bcl11b*$^{flox/+}$ mice as references. Average cell number is shown in the vicinity. CD4SP, CD4$^+$ single-positive; CD8SP, CD8$^+$ single-positive; DN, double-negative; DP, double-positive; ISP, immature single-positive; TCRβ, T-cell receptor-β.

premalignant thymocytes in cells before the DP stage. The result is of interest because thymic lymphomas in T-ALL mouse models having mutation in the *Ku70*, *FBXW7*, or *Pten* genes consisted of DP cells.[16–19] Furthermore, DP cells are assumed to be the origin of leukemia stem cells in *Pten*-null mice.[19]

Individual C-type thymocytes possessed common rearrangement sites at the *TCRβ* locus but underwent rearrangement at various different sites at the *TCRα* locus. This suggests the existence of a subpopulation of precursors within the C-type thymocytes that retains the capability of DNA rearrangement at the DP stage to produce cells with different TCRα chains.

© 2013 Japanese Cancer Association

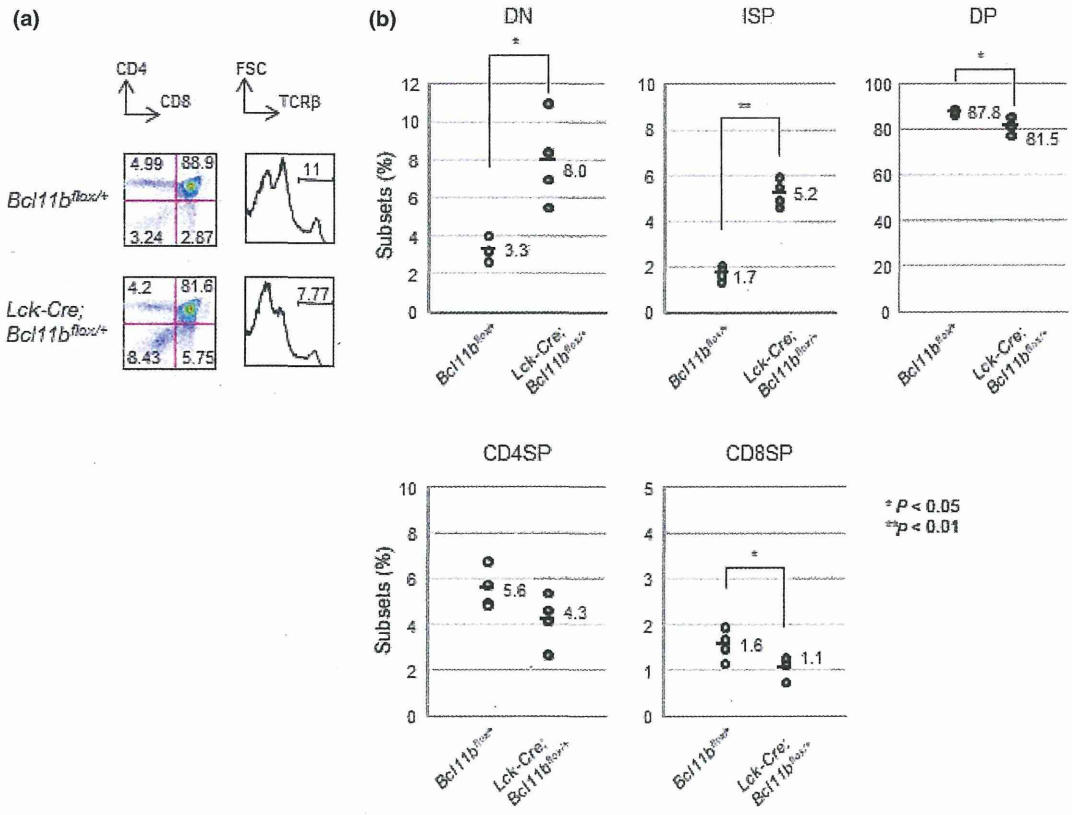

Fig. 5. Differentiation of thymocytes in *Bcl11b*$^{flox/+}$;*Lck-Cre* mice. (a) Flow cytometric analyses of thymocytes using CD4, CD8, and T-cell receptor-β (TCRβ) markers indicated above the panels. (b) Graphs show the percentage of indicated subsets in *Bcl11b*$^{flox/+}$ and *Bcl11b*$^{flox/+}$;*Lck-Cre* mice. CD4SP, CD4$^+$ single-positive; CD8SP, CD8$^+$ single-positive; DN, double-negative; DP, double-positive; ISP, immature single-positive.

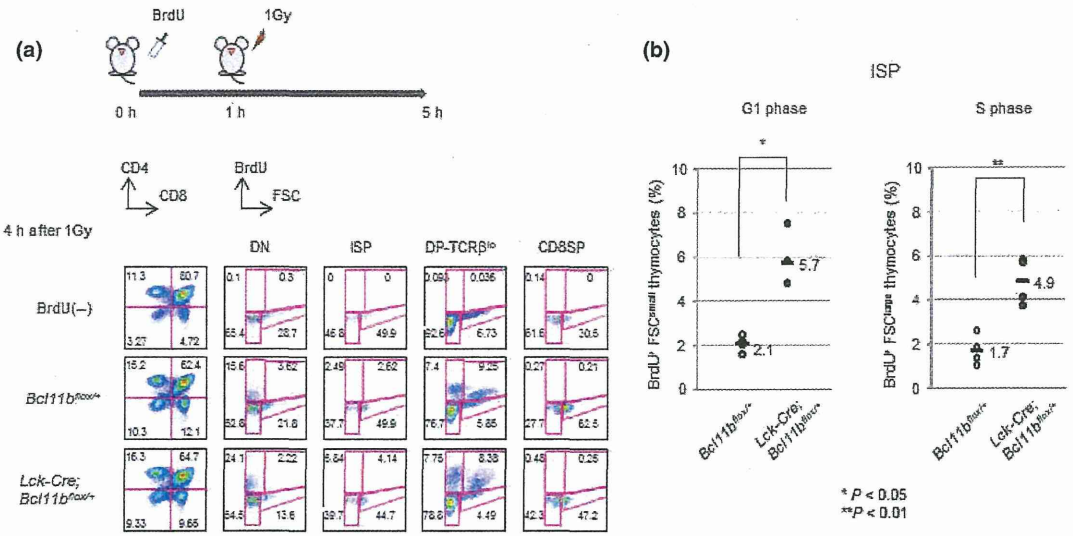

Fig. 6. Radiation effect on cell cycle in *Bcl11b*$^{flox/+}$;*Lck-Cre* mice. (a) Diagram depicts the time course after BrdU injection and γ-ray irradiation. Left panels show flow cytometric analyses of thymocytes using CD4 and CD8 markers. The other panels show flow cytometric analyses of BrdU incorporation levels (vertical axis) and forward scatter (FSC) values (horizontal axis) in thymocyte subsets in non-irradiated and irradiated *Bcl11b*$^{flox/+}$ and *Bcl11b*$^{flox/+}$;*Lck-Cre* mice. BrdU$^+$FSC^{large} fraction (right upper area) represents cells in S and G_2/M phases of the cell cycle, whereas BrdU$^+$FSC^{small} fraction (left upper quadrant) represents G_1 cells that have passed S phase. (b) Percentages of BrdU$^+$FSC^{small} cells (left) and BrdU$^+$FSC^{large} cells (right) in the immature single-positive (ISP) subset. CD8SP, CD8$^+$ single-positive; DN, double-negative; DP-TCRβ, double-positive T-cell receptor-β.

The C-type precursors are cells after the rearrangement at the *TCRβ* locus and before the rearrangement at the *TCRα* locus. Hence, they may be the immature cells present during the DN3 to DP stages, including ISP cells. However, the majority of C-type thymocytes showed committed or more mature phenotypes after the DP TCRβ^{low} stage, and a higher expression of TCRβ and CD8. This suggests that the C-type precursors continuously produce C-type thymocytes with differentiated

doi: 10.1111/cas.12193
© 2013 Japanese Cancer Association

phenotypes. In terms of proliferation and producing differentiated cells, the C-type precursors resemble, although are not parallel to, the premalignant DN3 cells that develop in *Lmo2*-transgenic mice,[15] as briefly described above. The *Lmo2*-DN3 cells give rise to thymic lymphomas after a long latency, and when transplanted, they develop DN3 cells within the recipient thymus that function for the bone marrow stem cells, continuously producing differentiated thymocytes. In contrast, transplanted *Bcl11b*$^{KO/+}$ premalignant immature cells were able to form thymic lymphomas, as shown in other premalignant immature thymocytes,[2,3] but were not able to produce committed DP thymocytes (Fig. S5). This suggests that acquisition of an *Lmo2*-transgene, but not loss of one *Bcl11b* allele, confers the stem cell-like property to DN cells.

The *Lck-Cre*-induced loss of one *Bcl11b* allele in thymocytes provided two- or three-fold elevation in the percentage of immature thymocytes, indicating the increase in cells of origin of the premalignant thymocytes described above. Therefore, this increase may be a contribution of the loss of one *Bcl11b* allele to thymic lymphoma development. Another contribution may be deregulation of the cell cycle. The ISP cells showed attenuation of arrest at S phase in *Bcl11b*$^{flox/+}$;*Lck-Cre* mice after γ-irradiation. This propensity of attenuation may influence the response to DNA damage and DNA replication stress, leading to genomic instability in thymocytes. Increased genomic instability is a key risk factor for leukemic transformation.[27,28] Consistent with this, a similar attenuated response was detected in *Bcl11b*$^{KO/+}$ mice.[26] One of the targets of Bcl11b transcription repressor is the *MDM2* gene, which functions as a negative regulator of p53, a key tumor suppressor.[29] Thus, loss of one *Bcl11b* allele may affect the p53–MDM2 feedback loop to reduce the p53 expression level.

Clonally expanding thymocytes were detected in *Bcl11b*$^{KO/+}$ mice of (MSM/Ms × BALB/c) F_1 genetic background at 60 and 80 days after 3 Gy γ-irradiation.[14] They also showed a decrease in the number of thymocytes, suggesting a relationship between C-type cell generation and the cell number decrease. This is consistent with the interpretation by classic histological studies that the tumors arose in small, lymphocyte-depleted thymuses.[25] However, the C-type thymocytes differ in phenotype from those in irradiated *Bcl11b*$^{flox/+}$;*Lck-Cre* mice. One difference is that most C-type thymocytes consisted of immature cells but not mature thymocytes highly expressing TCRβ, indicating differentiation arrest of thymocytes before the DP stage. Another difference is the decrease in cell proliferation. In *Bcl11b*$^{KO/+}$ mice, loss of one *Bcl11b* allele exists in almost all cells of T-cell lineage in the thymus, whereas in *Bcl11b*$^{flox/+}$;*Lck-Cre* mice the loss occurs only in thymocytes after the DN2/DN3 stages. Although some of these differences may have been attributable to the different genetic background of the mice used, the results suggest that loss of one *Bcl11b* allele in different thymocyte subsets leads to premalignant cells with different properties, and that the origin of premalignant thymocytes can be cells at different developmental stages depending on the stage of the driver mutation.

These findings may parallel, in part, results published in a recent report that tests the effect of cell of origin on thymic lymphoma development by using three different *Cre*-transgenic mouse strains carrying *Vav-1-Cre*, *Lck-Cre*, and *CD4-Cre*.[30] The strains can induce Sleeping Beauty transposase expression at three different developmental stages, leading to insertional mutagenesis in different types of thymocytes or their progenitors. All three strains developed thymic lymphomas, and the thymic lymphomas showed different latencies and different distributions of driver mutations in the three strains. Although phenotypes of the thymic lymphomas were not examined, the study shows that the cell of origin is a key determinant of the effectiveness and genetic selection in thymic lymphoma development.

Acknowledgments

This work was supported by grants-in-aid of the Third Term Comprehensive Control Research for Cancer from the Ministry of Health, Labor and Welfare of Japan, and for Cancer Research from the Ministry of Education, Science, Technology, Sports, and Culture of Japan.

Disclosure Statement

The authors have no conflict of interest.

References

1 Kaplan HS, Carnes WH, Brown MB, *et al.* Indirect induction of lymphomas in irradiated mice. I. Tumor incidence and morphology in mice bearing non-irradiated thymic grafts. *Cancer Res* 1956; **16**: 422–5.
2 Muto M, Kubo E, Sado T. Development of prelymphoma cells committed to thymic lymphomas during radiation-induced thymic lymphomagenesis in B10 mice. *Cancer Res* 1987; **47**: 3469–72.
3 Sado T, Kamisaku H, Kubo E. Bone marrow-thymus interactions during thymic lymphomagenesis induced by fractionated radiation exposure in B10 mice: analysis using bone marrow transplantation between Thy 1 congenic mice. *J Radiat Res* 1991; **32**: 168–80.
4 Kominami R, Niwa O. Radiation carcinogenesis in mouse thymic lymphomas. *Cancer Sci* 2006; **97**: 575–81.
5 Armstrong SA, Look AT. Molecular genetics of acute lymphoblastic leukemia. *J Clin Oncol* 2005; **23**: 6306–15.
6 Paganin M, Ferrando A. Molecular pathogenesis and targeted therapies for NOTCH1-induced T-cell acute lymphoblastic leukemia. *Blood Rev* 2011; **25**: 83–90.
7 Kominami R. Role of the transcription factor Bcl11b in development and lymphomagenesis. *Proc Jpn Acad Ser B Phys Biol Sci* 2012; **88**: 72–87.
8 Wakabayashi Y, Inoue J, Takahashi Y, *et al.* Homozygous deletions and point mutations of the Rit1/Bcl11b gene in gamma-ray induced mouse thymic lymphomas. *Biochem Biophys Res Commun* 2003; **301**: 598–603.
9 Wakabayashi Y, Watanabe H, Inoue J, *et al.* Bcl11b is required for differentiation and survival of αβT lymphocytes. *Nat Immunol* 2003; **4**: 533–9.
10 Keersmaecker K, Real PJ, Gatta GD, *et al.* The TLX1 oncogene drives aneuploidy in T cell transformation. *Nat Med* 2010; **16**: 1321–7.
11 Kamimura K, Ohi H, Kubota T, *et al.* Haploinsufficiency of Bcl11b for suppression of lymphomagenesis and thymocyte development. *Biochem Biophys Res Commun* 2007; **355**: 538–42.
12 Gutierrez A, Kentsis A, Sanda T, *et al.* The BCL11B tumor suppressor is mutated across the major molecular subtypes of T-cell acute lymphoblastic leukemia. *Blood* 2011; **118**: 4169–73.
13 Ohi H, Mishima Y, Kamimura K, Maruyama M, Sasai K, Kominami R. Multi-step lymphomagenesis deduced from DNA changes in thymic lymphomas and atrophic thymuses at various times after γ-irradiation. *Oncogene* 2007; **26**: 5280–9.
14 Go R, Hirose S, Morita S, *et al.* Bcl11b heterozygosity promotes clonal expansion and differentiation arrest of thymocytes in gamma-irradiated mice. *Cancer Sci* 2010; **101**: 1347–53.
15 McCormack MP, Young LF, Vasudevan S, *et al.* The *Lmo2* Oncogene Initiates Leukemia in Mice by Inducing Thymocyte Self-Renewal. *Science* 2010; **327**: 879–83.
16 Li GC, Ouyang H, Li X, *et al.* Ku70: a candidate tumor suppressor gene for murine T cell lymphoma. *Mol Cell* 1998; **2**: 1–8.
17 Onoyama I, Tsunematsu R, Matsumoto A, *et al.* Conditional inactivation of Fbxw7 impairs cell-cycle exit during T cell differentiation and results in lymphomatogenesis. *J Exp Med* 2007; **204**: 2875–88.
18 Xue L, Nolla H, Suzuki A, *et al.* Normal development is an integral part of tumorigenesis in T cell-specific PTEN-deficient mice. *Proc Natl Acad Sci U S A* 2008; **105**: 2022–7.
19 Guo W, Schubbert S, Chen JY, *et al.* Suppression of leukemia development caused by PTEN loss. *Proc Natl Acad Sci U S A* 2011; **108**: 1409–14.
20 Takahama Y, Ohishi K, Tokoro Y, *et al.* Functional competence of T cells in the absence of glycosylphosphatidylinositol-anchoredproteins caused by T cell-specific disruption of the Pig-a gene. *Eur J Immunol* 1998; **28**: 2159–66.

© 2013 Japanese Cancer Association

21 Lee PP, Fitzpatrick DR, Beard C, *et al.* A critical role for Dnmt1 and DNA methylation in T cell development, function, and survival. *Immunity* 2001; **15**: 763–74.
22 Kawamoto H, Ohmura K, Fujimoto S, *et al.* Extensive proliferation of T cell lineage-restricted progenitors in the thymus: an essential process for clonal expression of diverse T cell receptor beta chains. *Eur J Immunol* 2003; **33**: 606–15.
23 Hu T, Simmons A, Yuan J, *et al.* The transcription factor c-Myb primes CD4+CD8+ immature thymocytes for selection into the iNKT lineage. *Nat Immunol* 2010; **11**: 435–41.
24 Fischer A, Malissen B. Natural and engineered disorders of lymphocyte development. *Science* 1998; **280**: 237–43.
25 Siegler R, Harrwll W, Rich MA. Pathogenesis of radiation-induced thymic lymphoma in mice. *J Natl Cancer Inst* 1966; **37**: 105–21.
26 Go R, Takizawa K, Hirose S, *et al.* Impairment in differentiation and cell cycle of thymocytes by loss of a Bcl11b tumor suppressor allele that contributes to leukemogenesis. *Leuk Res* 2012; **36**: 1035–40.
27 Bartkova J, Horejsi Z, Koed K, *et al.* DNA damage response as a candidate anti-cancer barrier in early human tumorigenesis. *Nature* 2005; **434**: 864–70.
28 Gorgoulis VG, Vassiliou LV, Karakaidos P, *et al.* Activation of the DNA damage checkpoint and genomic instability in human precancerous lesions. *Nature* 2005; **434**: 907–13.
29 Obata M, Kominami R, Mishima Y. BCL11B tumor suppressor inhibits HDM2 expression in a p53-dependent manner. *Cell Signal* 2012; **24**: 1047–52.
30 Berquam-Vrieze KE, Nannapaneni K, Brett BT, *et al.* Cell of origin strongly influences genetic selection in a mouse model of T-ALL. *Blood* 2011; **118**: 4646–56.

Supporting Information

Additional Supporting Information may be found in the online version of this article:

Fig. S1. Analysis of deletion of Bcl11b floxed allele in *Bcl11b*$^{flox/+}$;*Lck-Cre* and *Bcl11b*$^{flox/+}$;*CD4-Cre* mice.

Fig. S2. Analysis of lymphoma-bearing *Bcl11b*$^{flox/+}$;*Lck-Cre* mice.

Fig. S3. Differentiation of thymocytes in *Bcl11b*$^{flox/+}$;*CD4-Cre* mice 60 days after 3 Gy γ-irradiation.

Fig. S4. Differentiation of thymocytes in *Bcl11b*$^{flox/+}$;*CD4-Cre* mice.

Fig. S5. Analysis of thymocytes in recipient mice after cell transplantation.

doi: 10.1111/cas.12193
© 2013 Japanese Cancer Association

Biochemical and Biophysical Research Communications 432 (2013) 34–39

Contents lists available at SciVerse ScienceDirect

Biochemical and Biophysical Research Communications

journal homepage: www.elsevier.com/locate/ybbrc

Arf and p53 act as guardians of a quiescent cellular state by protecting against immortalization of cells with stable genomes

Tomoyuki Osawa [a,b,1], Yuko Atsumi [a,c,1], Eiji Sugihara [d], Hideyuki Saya [d], Masamoto Kanno [e], Fumio Tashiro [b], Mitsuko Masutani [a], Ken-ichi Yoshioka [a,*]

[a] Division of Genome Stability Research, National Cancer Center Research Institute, 5-1-1 Tsukiji, Chuo-ku, Tokyo 104-0045, Japan
[b] Biological Science and Technology, Tokyo University of Science, 2641 Yamazaki, Noda 278-8510, Japan
[c] Department of Biosciences, School of Science, Kitasato University, 1-15-1 Kitasato, Minami-ku, Sagamihara 252-0373, Japan
[d] Division of Gene Regulation, School of Medicine, Keio University, 35 Shinanomachi, Shinjuku-ku, Tokyo 160-8582, Japan
[e] Department of Immunology, Graduate School of BioMedical & Health Sciences, Hiroshima University, 1-2-3 Kasumi, Minami-ku, Hiroshima 734-8551, Japan

ARTICLE INFO

Article history:
Received 21 January 2013
Available online 31 January 2013

Keywords:
Arf
Genome stability
H2AX
p53
Quiescent state

ABSTRACT

Normal cells undergo a growth-arrested status that is produced by p53-dependent down-regulation of histone H2AX. Immortality is developed after abrogation of the H2AX-diminished state, which is associated with genomic instability (often with tetraploidy) and the induction of mutations in either the *Arf* or *p53* gene. However, the role of Arf in control of H2AX expression and genome stability is still unclear. Here, we show that both Arf and p53 are required for the down-regulation of H2AX and formation of the growth-arrested state. Wild-type (WT) mouse embryonic fibroblasts (MEFs) subjected to tetraploidization with DNA lesions did not undergo mitotic catastrophe-associated cell death and stayed in a growth-arrested state, until immortality was attained with mutations in the *Arf/p53* module and recovery of H2AX expression. Whereas tetraploidization was essential for immortalization of WT MEFs, this event was not required for immortalization of MEFs containing mutations in *Arf/p53* and these cells still underwent mitotic catastrophe-associated cell death. Thus, WT MEFs are protected from immortalization with genome stability, which is abrogated with tetraploidization and mutation of either *Arf* or *p53*.

© 2013 Elsevier Inc. All rights reserved.

1. Introduction

Most cancers that develop in old age are characterized by chromosomal or microsatellite instabilities, as well as mutations in genes, such as those involved in the Arf-MDM2-p53 axis [1–3]. Similar to cancer cells, mouse embryonic fibroblasts (MEFs) acquire immortality associated with genomic instability [4] and mutations in the *Arf/p53* module [5]. Although *Arf* and *p53* are part of the same regulatory module, these genes are mutated in a mutually exclusive manner in immortalized MEFs, suggesting that both Arf and p53 are required for protection against cellular immortalization [6,7]. By contrast, the p53-dependent acute response to damage still occurs in p53-proficient cancer cells that contain mutations in *Arf* [8,9]. These findings suggest that normal cells are protected from immortalization by regulation of both Arf and p53, and that this protection mechanism is distinct from the role of p53 in the acute damage response [6].

Because Arf and p53 are critical tumor suppressors, *Arf*- and *p53*-knockout (KO) mice are predisposed to cancer development [10,11]. In addition, transgenic mice with an extra copy of the *Arf* and *p53* genes (super-*Arf/p53* mice) show signs of cancer suppression and have extended life spans [5]. Intriguingly, like wild-type MEFs with stable genomes, MEFs from super-*Arf/p53* mice are strongly protected against immortalization [5]. These findings imply that the primary function of the Arf/p53 module is control of cellular homeostasis, which contributes to lifespan extension and cancer suppression. By contrast, cells with hyperactive p53 induced by overexpression or acute damage undergo senescence or apoptosis *in vitro* [12–14], and transgenic mice with hyperactive p53 undergo premature aging [15–17]. Furthermore, mutant mice that are unable to induce many of the canonical p53 target genes in response to acute DNA damage retain tumor suppression activity under normal conditions [8,9]. Taken together, these findings suggest that p53 has distinct functions under normal and hyperactivated conditions; the Arf-dependent function of p53 is to control cellular homeostasis under normal conditions, leading to lifespan extension and cancer prevention, and is likely to be distinct from the function of hyperactivated p53 [6].

After serial proliferation, normal cells generally undergo a growth-arrested state associated with diminished levels of H2AX

Abbreviations: CTU, camptothecin; HU, hydroxyurea; KO, knockout; MEFs, mouse embryonic fibroblasts; WT, wild-type.

* Corresponding author. Fax: +81 3 3543 9305.
E-mail address: kyoshiok@ncc.go.jp (K.-i. Yoshioka).

[1] These authors contributed equally to this work.

0006-291X/$ - see front matter © 2013 Elsevier Inc. All rights reserved.
http://dx.doi.org/10.1016/j.bbrc.2013.01.091

[6,7]. These growth-arrested cells are defective in DNA damage repair and are therefore susceptible to the accumulation of unrepaired DNA lesions [18]. In response to aberrantly accelerated growth stimuli, these growth-arrested cells develop DNA replication stress-associated lesions and subsequent genomic instability [4]. Cellular growth retardation and DNA damage repair deficiency are both likely caused by a reduction in histone H2AX levels because cells lacking H2AX also display these characteristics [19–22]. By contrast, transformed or immortalized cells are formed following abrogation of the H2AX-diminished state [6,7].

Down-regulation of H2AX is dependent on p53; the mechanism of regulation presumably involves the Arf/p53 module because the H2AX-diminished and growth-arrested state is not induced in *p53*-KO MEFs or in immortalized MEFs that contain mutations in either *Arf* or *p53* [6,7]. Although the role of p53 in establishment of a quiescent state has been described previously [6,7], the mechanism by which Arf contributes to the down-regulation of H2AX, protection against immortalization, and genomic instability (ploidy) is still unclear.

In this study, we demonstrate that Arf is required for growth arrest associated with reduced levels of H2AX in MEFs. The quiescent state of normal MEFs was abrogated by mutations in either *Arf* or *p53*. Although tetraploidization was not essential for immortalization of *p53*-KO and *Arf*-KO MEFs, tetraploidization of wild-type (WT) MEFs was required to induce mutations in the Arf/p53 module.

2. Materials and methods

2.1. Cell culture

WT, *Arf*-KO, and *p53*-KO MEFs were prepared from Day 13.5 mouse embryos, as previously described [7]. MEFs were cultured as described previously [23] and were passaged using the standard 3T3 protocol [24], unless otherwise indicated. DNA replication stress-associated damage was induced by the treatment of cells with camptothecin (CPT) (Sigma) or hydroxyurea (HU) (Sigma) as indicated in each figure.

2.2. Antibodies and immunoblotting

Antibodies against H2AX (Bethyl Laboratories), γH2AX (Millipore-Upstate), β-actin (AC-74, Sigma), Parp1 (Cell Signaling Technology), cleaved caspase-3 (Cell Signaling Technology), and histone H3 (MABI0301, Monoclonal Antibody Institute) were used in this study. Immunoblotting was performed as described previously [23].

2.3. Analyses of the chromosomal status

For analyses of mitotic phase chromosomes, cells were treated with 200 ng/ml nocodazole for 5 h and then mitotic cells were collected. The cells were hypotonically swollen by treatment with 75 mM KCl for 30 min, and then fixed with Carnoy's solution (60% methanol, 30% acetic acid, and 10% chloroform) for 20 min. After changing the fixative once, cells were dropped onto glass slides and air-dried [4]. The slides were stained with 4% Giemsa stain (Merck) for 10 min, washed briefly in tap water, and then air-dried. For FACS analyses of the cellular ploidy status, harvested cells were incubated in PBS containing RNase A (200 μg/ml, Sigma) for 30 min on ice and then stained with propidium iodide (20 μg/ml, Sigma) for an additional 30 min on ice in the dark. The stained cells were analyzed by flow cytometry (Beckman Coulter).

3. Results

3.1. Arf-KO MEFs do not undergo H2AX-diminished growth arrest

To determine the role of Arf in the establishment of a H2AX-diminished and growth-arrested state, experiments were performed using primary WT and *Arf*-KO MEFs. Unlike WT MEFs, the *Arf*-KO MEFs did not undergo growth arrest and continued to

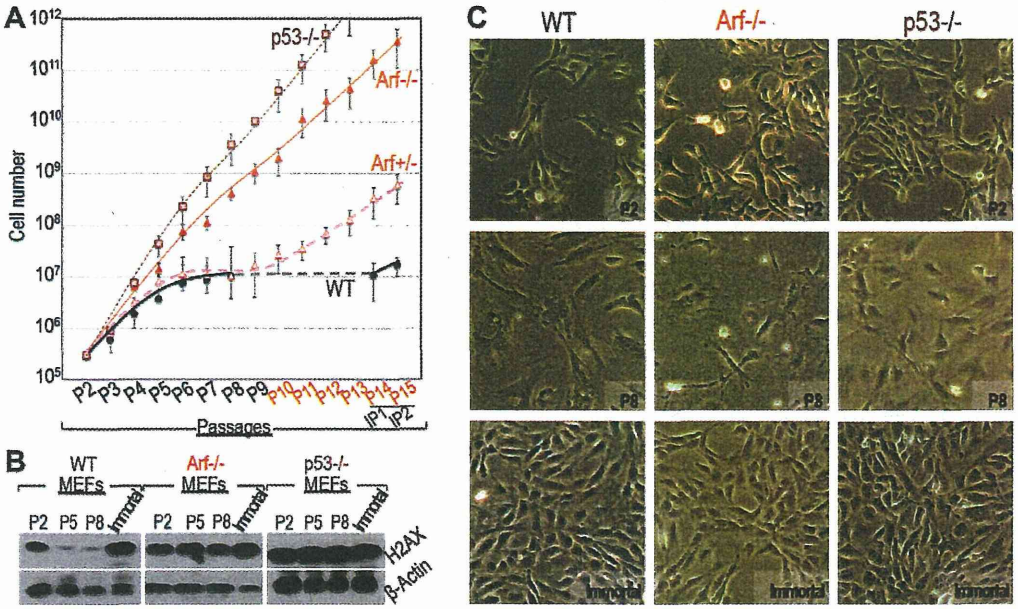

Fig. 1. Arf-KO MEFs do not undergo H2AX-diminished growth arrest. (A) Growth curves of MEFs (WT, $Arf^{+/-}$, $Arf^{-/-}$, and $p53^{-/-}$) cultured under a standard 3T3 passage protocol. Unlike WT and $Arf^{+/-}$ MEFs, $Arf^{-/-}$ MEFs continuously grew and developed immortality. Data show the mean ± SD of $n = 3$ independent experiments. IP1 and IP2 indicate Immortal Passage 1 and 2 for WT MEFs. (B) Immunoblot analysis of histone H2AX expression in passage 2 (P2), P5, P8, and immortalized MEFs (WT, $Arf^{-/-}$, and $p53^{-/-}$). Expression levels of β-actin were used as a loading control. Unlike WT MEFs, $Arf^{-/-}$ and $p53^{-/-}$ MEFs failed to form the H2AX-diminished state. (C) Morphologies of P2, P8, and immortalized WT, $Arf^{-/-}$, and $p53^{-/-}$ MEFs. Similar to WT MEFs, $Arf^{-/-}$ and $p53^{-/-}$ MEFs displayed a senescent morphology before acquiring the immortalized morphology.

immortalize across 15 passages (Fig. 1A); this result is consistent with a previous report [11] and with the growth of *p53*-KO MEFs. In addition, immunoblot analyses revealed that expression levels of H2AX in the *Arf*-KO MEFs and *p53*-KO MEFs were not down-regulated across multiple passages (Fig. 1B). These data support the notion that the establishment of an H2AX-diminished and growth-arrested state in normal cells is regulated by both Arf and p53, and that this state is abrogated by genomic instability caused by mutations in the Arf/p53 module.

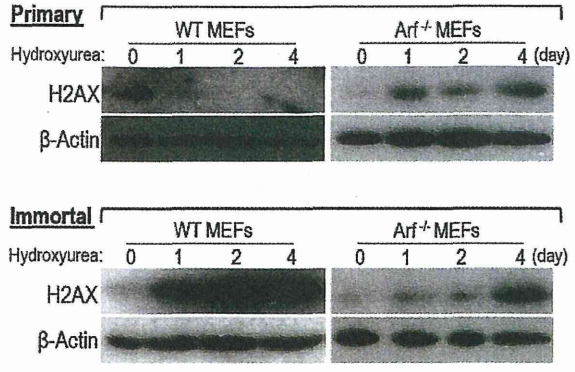

Fig. 2. DNA replication stress-induced down-regulation of H2AX is dependent on Arf. DNA replication stress was induced in primary and immortalized WT and $Arf^{-/-}$ MEFs by treatment with 0.2 mM HU for up to 4 days. The DNA replication stress-induced down-regulation of H2AX was abrogated in immortalized WT MEFs and in both primary and immortalized $Arf^{-/-}$ MEFs.

In spite of the lack of growth arrest, the flattened and enlarged cellular morphology of both *p53*-KO and *Arf*-KO MEFs was similar to that of the senescent WT MEFs. The immortalized KO cells subsequently acquired the morphology typically seen in immortalized MEFs (Fig. 1C). This result indicates that both Arf and p53 are required for the establishment of the H2AX-diminished state but are not essential for the formation of some of the typical senescent characteristics of the cells, including the flattened and enlarged morphology. In addition, since growth retardation is observed following knockdown of H2AX [7,19], Arf- and p53-dependent diminution of H2AX is likely a direct cause of the growth-arrested state of normal cells.

To examine the effect of Arf on the down-regulation of H2AX directly, DNA replication stress was induced in WT and *Arf*-KO MEFs by exposing cells to HU that depletes dNTP pool. The expression level of H2AX in *Arf*-KO MEFs was compared with that in WT MEFs because H2AX is down-regulated during DNA replication stress in WT MEFs but not in *p53*-KO MEFs. As expected, H2AX expression was down-regulated in primary WT MEFs after 1–4 days of treatment with HU. By contrast, H2AX expression was not down-regulated in immortalized WT MEFs, primary *Arf*-KO MEFs, or immortalized *Arf*-KO MEFs (Fig. 2); this result agrees with a previous report of stable H2AX expression in DNA replication stress-induced *p53*-KO MEFs [7]. These data further support the proposal

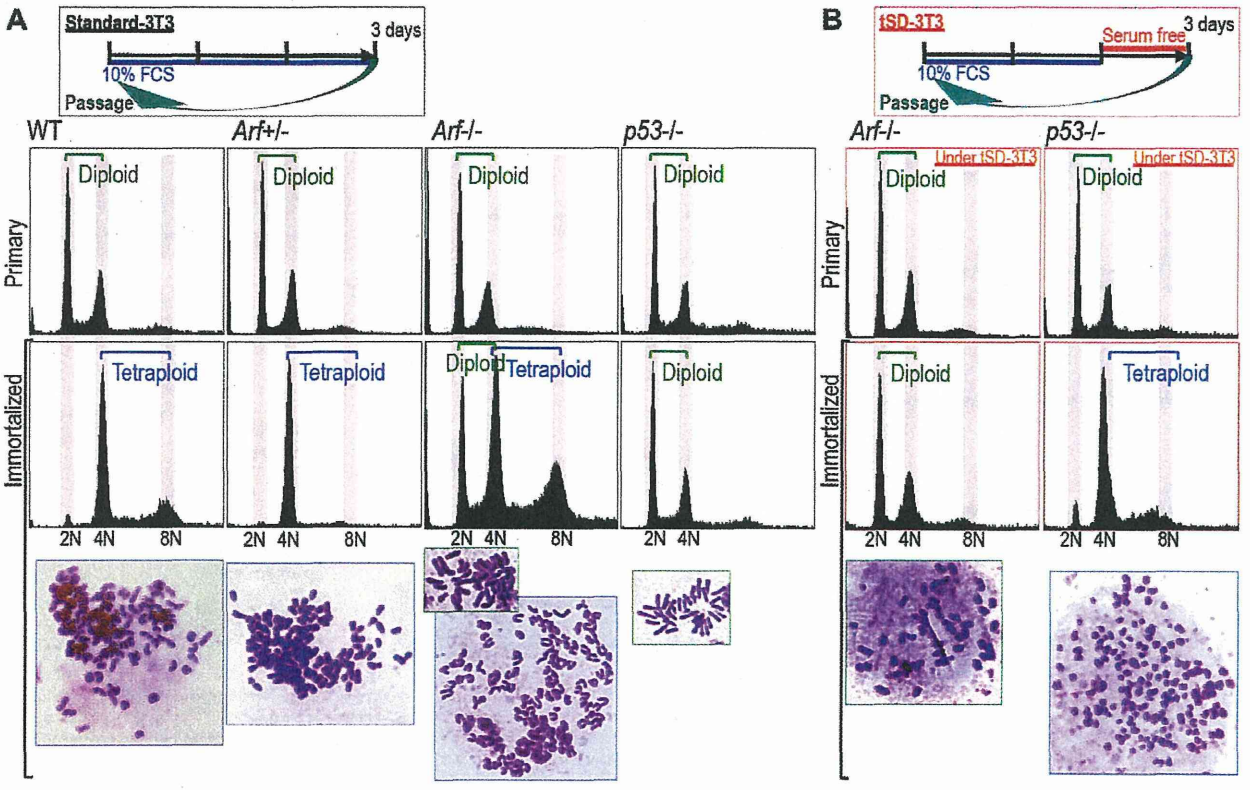

Fig. 3. Tetraploidization is not essential for immortalization of $Arf^{-/-}$ and $p53^{-/-}$ MEFs. (A) FACS analyses of changes in the cellular ploidy status of primary and immortalized WT, $Arf^{+/-}$, $Arf^{-/-}$, and $p53^{-/-}$ MEFs cultured under standard 3T3 conditions. WT and $Arf^{+/-}$ MEFs showed tetraploidization after development of immortality, while $p53^{-/-}$ MEFs immortalized with diploidy. Immortalized $Arf^{-/-}$ MEFs were a mixture of dipoid and tetraploid states. Giemsa stains of M-phase chromosomes are also shown. Images are the representatives (diploidy with green frame and tetraploidy with blue frame). (B) FACS analyses of changes in the cellular ploidy status of $Arf^{-/-}$ and $p53^{-/-}$ MEFs during culture under growth-restricted tSD-3T3 conditions. Under these conditions, $Arf^{-/-}$ MEFs immortalized with diploidy, whereas immortalized $p53^{-/-}$ MEFs developed tetraploidy. Giemsa stains of M-phase chromosomes are also shown. (For interpretation of the references to colour in this figure legend, the reader is referred to the web version of this article.)

that the H2AX-diminished and growth-arrested state of normal cells is dependent on both Arf and p53, and that this quiescent state is abrogated by knockout of the Arf/p53 module, which causes recovery of H2AX expression and subsequent growth activity.

3.2. Immortalized *Arf*-KO MEFs are a mixture of diploid and tetraploid cells

In WT MEFs, mutation of the Arf/p53 module is induced during tetraploidization and leads to the recovery of H2AX expression and development of immortality [7]. By contrast, *p53*-KO MEFs maintain a stable diploid state even after immortalization [7]. These previous observations motivated us to examine the genomic status of *Arf*-KO MEFs during immortalization. FACS analysis revealed that immortalized *Arf*-KO MEFs were a mixture of tetraploid and diploid states (Fig. 3A). Giemsa staining also showed that the M-phase chromosomes of immortalized *Arf*-KO MEFs were a mixture of two types: one similar to the chromosomes of immortalized WT MEFs and another similar to those of immortalized *p53*-KO MEFs (Fig. 3A). Since *p53*-KO and *Arf*-KO MEFs acquired immortality with diploidy (at least partly in the case of *Arf*-KO MEFs), these findings suggest that tetraploidization is not essential for immortalization in an *Arf*-mutated or *p53*-mutated background.

To address whether the tetraploidization of *Arf*-KO MEFs is induced in a similar manner to that of WT MEFs, *Arf*-KO MEFs were continuously cultured under a 3T3 passage protocol with temporary depletion of serum for the day immediately prior to passage (tSD-3T3). Under these conditions, tetraploidization of immortalized WT MEFs is neutralized and cells are continuously growth arrested with stable diploidy [7]. Tetraploidization of immortalized *Arf*-KO MEFs was also inhibited when cells were cultivated under the tSD-3T3 conditions (Fig. 3B); this result confirms the hypothesis that tetraploidization is not required for immortalization in an *Arf*-mutated background. In addition, these results indicate that MEFs lacking Arf develop tetraploidy in response to accelerated growth stimuli, although this tetraploidization does not affect growth activity or immortalization.

3.3. Immortalized *p53*-KO MEFs cultured under growth-restricted conditions develop tetraploidy

Under standard 3T3 culture conditions, *p53*-KO MEFs maintained a diploid status during immortalization (Fig. 3A); however, these cells developed tetraploidy under growth-restricted (tSD-3T3) conditions (Fig. 3B). This result was unexpected because tetraploidization of the *Arf*-KO MEFs was inhibited under the tSD-3T3 conditions. Although the mechanism by which tetraploidization is induced in *p53*-KO MEFs is unclear, this event may be associated with oxidative stress because the level of reactive oxygen species is elevated during serum depletion [25,26]. Although

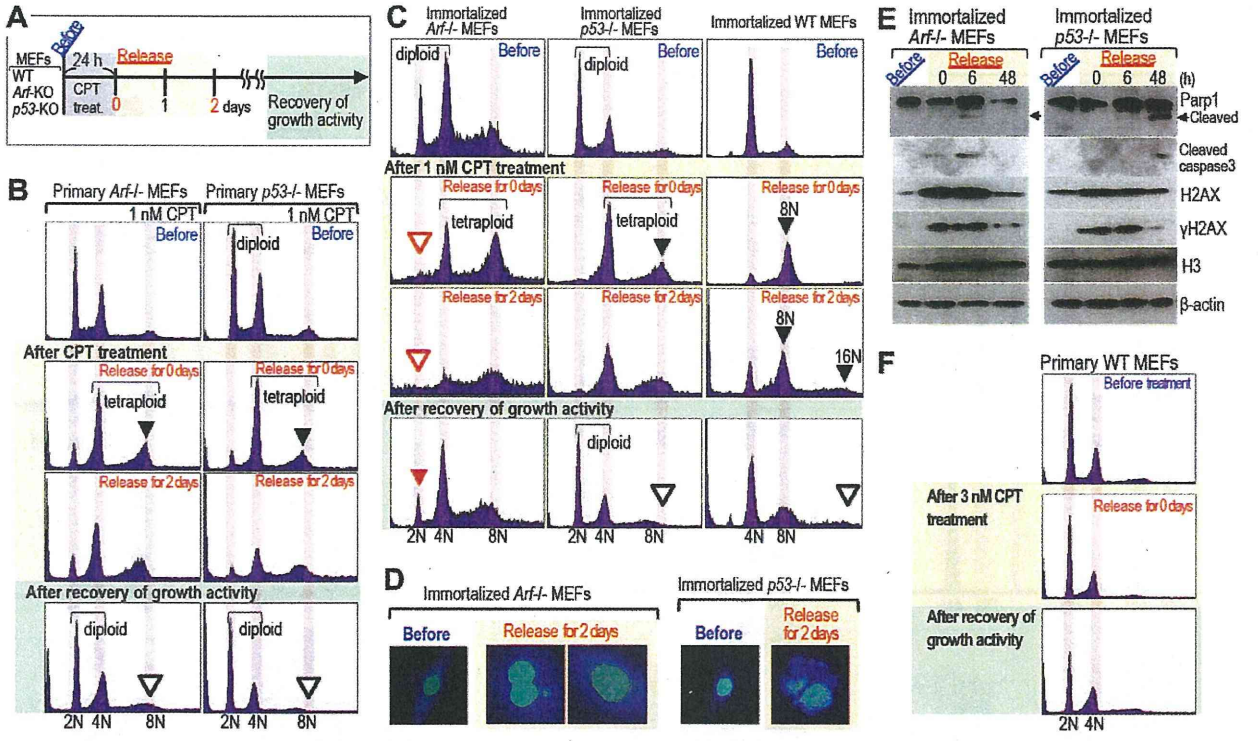

Fig. 4. Sensitivity to mitotic catastrophe affects the ploidy status of WT, $Arf^{-/-}$, and $p53^{-/-}$ MEFs. (A) WT, $Arf^{-/-}$, and $p53^{-/-}$ MEFs were exposed to CPT for 24 h and then released from treatment to induce mitotic catastrophe and to determine the effect on induction of cell death. (B) FACS analyses of primary $Arf^{-/-}$ and $p53^{-/-}$ MEFs before and after CPT treatment, and during growth recovery. These cells developed tetraploidy following exposure to CPT (solid black arrowhead) and the tetraploid cells selectively died via mitotic catastrophe during growth recovery (open black arrowheads). (C) FACS analyses of immortalized WT, $Arf^{-/-}$, and $p53^{-/-}$ MEFs before and after CPT treatment, and during growth recovery. Similar results to those seen for the primary KO MEFs were observed. In immortalized $Arf^{-/-}$ MEFs, which were a mixture of diploid and tetraploid cells (2N, 4N, and 8N chromosomes), the 2N peak was reduced following CPT treatment (open red arrowhead) and increased again upon growth recovery (solid red arrowhead). (D) Representative nuclei staining of immortalized $Arf^{-/-}$ and $p53^{-/-}$ MEFs before exposure to CPT and after release for 2 days. Multinucleated cells, which are typically formed during mitotic catastrophe cell death, were observed in $p53^{-/-}$ MEFs but not in $Arf^{-/-}$ MEFs. (E) Immunoblot analyses of the expression levels of Parp1, cleaved Parp1, caspase-3, cleaved caspase-3, H2AX, γH2AX, and histone H3 in immortalized $Arf^{-/-}$ and $p53^{-/-}$ MEFs before exposure to CPT and after release for 0 h, 6 h, or 48 h. Expression levels of β-actin were measured as a loading control. (F) FACS analysis of the ploidy status of primary WT MEFs before and after exposure to CPT. Unlike $Arf^{-/-}$ and $p53^{-/-}$ MEFs, primary WT MEFs did not undergo mitotic catastrophe or growth arrest. (For interpretation of the references to colour in this figure legend, the reader is referred to the web version of this article.)

tetraploidization could be induced in both *Arf*-KO and *p53*-KO MEFs (dependent on the culture conditions), this response was not associated with the development of immortality. By contrast, mutation of the *Arf/p53* module in WT MEFs is induced in association with tetraploidization [7].

3.4. Sensitivity to mitotic catastrophe determines the ploidy state of cells

In agreement with our recent study [4,7], the results described above indicate that tetraploidization is dispensable for immortalization of *Arf/p53*-mutated cells. Conversely, tetraploidization and associated mutation of the *Arf/p53* module are prerequisites for immortalization of WT MEFs, whereas cells in the diploid state are stably protected against immortalization [6]. However, the mechanisms by which tetraploidization of *p53*-KO MEFs is protected under growth-restricted conditions and by which tetraploidy of immortalized WT MEFs is preserved without the development of further polyploidy (such as 16N or 32N) are still unknown. The response to mitotic catastrophe, during which cells that contain DNA lesions are enter mitosis and die as they unable to maintain proper cell cycle arrest, is a mechanism that may be associated with these events [27]. Mitotic catastrophe is a major trigger of cancer cell death during treatment with anti-cancer drugs that damage DNA [28–31], whereas senescent WT MEFs with identical DNA lesions are able to progress through mitosis without undergoing cell death [4]. To investigate their sensitivity to mitotic catastrophe, MEFs were exposed to the topoisomerase I inhibitor CPT, which acts as an anti-cancer drug, and then released from treatment to induce mitotic catastrophe (Fig. 4A). Surviving cells were identified after growth-activity was recovered. FACS analysis revealed that primary *p53*-KO and *Arf*-KO MEFs underwent mitotic catastrophe with associated tetraploidization following CPT treatment (Fig. 4B, solid arrowheads). However, the 8N peak disappeared after growth recovery of these cells, indicating that the surviving cells were exclusively diploid (Fig. 4B, open arrowheads) and that selective mitotic catastrophe-associated death of the tetraploid cells had occurred.

Similar to the primary *p53*-KO and *Arf*-KO MEFs, immortalized *p53*-KO (diploid) and WT MEFs (tetraploid) underwent selective cell death via mitotic catastrophe (Fig. 4C, solid black arrowheads). For the immortalized *Arf*-KO MEFs, which were a mixture of diploid and tetraploid cells, the 2N peak disappeared after treatment with CPT (Fig. 4C, open red arrowheads) and then recovered in the surviving cells (Fig. 4C, filled red arrowhead), indicating that cells subjected to mitotic catastrophe underwent cell death. Formation of multinucleated cells, which are generally observed after mitotic catastrophe, was typically observed in immortalized *p53*-KO MEFs but not in immortalized *Arf*-KO MEFs (Fig. 4D). However, *Arf*-KO MEFs showed more efficient appearance of cleaved caspase-3 and cleaved Parp1 than *p53*-KO MEFs (Fig. 4E), suggesting efficient apoptosis induction in the *Arf*-KO MEFs. These data suggest that the mechanisms of cell death after mitotic catastrophe might be multiple and dependent on the mutation status of *Arf* and *p53*. Nevertheless, these results indicate that MEFs containing mutations of the *Arf/p53* module are highly sensitive to mitotic catastrophe, which impacts the resulting ploidy status of the cells. In fact, immortalized WT MEFs were exclusively tetraploid; therefore, mitotic catastrophe-associated cell death is probably one reason why these cells do not undergo further polyploidy (such as 16N or 32N) (Fig. 4C).

In contrast to the primary *Arf*-KO and *p53*-KO MEFs, primary WT MEFs exposed to CPT did not display signs of mitotic catastrophe, tetraploidization, or G2/M cell cycle arrest (Fig. 4F). This result suggests that the sensitivity of primary WT MEFs to mitotic catastrophe-associated cell death differs from that of the cells containing mutations in the *Arf/p53* module.

4. Discussion

This study demonstrates that both Arf and p53 are required for the establishment of an H2AX-diminished and growth-arrested state in which cells are quiescent and protected against immortalization. The results presented here indicate that mutations in either *Arf* or *p53* induce recovery of H2AX expression and development of immortality. In spite of the lack of growth arrest of *Arf*-KO and *p53*-KO MEFs, the morphology of these cells was similar to that of senescent WT MEFs. Therefore, although the Arf/p53 module is required for the establishment of a growth-arrested state and down-regulation of H2AX, proper functioning of this regulatory module is not always associated with the senescent morphological characteristics of cells.

Together with the results of our previous studies [4,7,32], the data presented here demonstrate that the cellular ploidy status is determined by at least two distinct cellular events that occur during immortalization: (i) tetraploidization-coupled induction of mutations in the Arf/p53 module, which leads to immortalization of WT MEFs and (ii) mitotic catastrophe-associated cell death, which occurs in *Arf/p53* mutated cells but is not induced in normal MEFs. Senescent WT MEFs survive after mitotic catastrophe, causing tetraploidization with mutation induction in the *Arf/p53* module, whereas cells containing mutations in the *Arf/p53* module are more sensitive to mitotic catastrophe-induced cell death. Therefore, diploid cells are protected against immortalization but tetraploid immortalized cells do not usually show further ploidy (16N or 32N).

Because tetraploidization is caused by carryover of DNA lesions through mitosis [4], immortalized tetraploid MEFs are cells that escape cell death during mitotic catastrophe. Although the mechanism that determines whether cells either escape from or undergo mitotic catastrophe-related cell death is currently unclear, tetraploid primary WT MEFs survive under accelerated growth stimuli; therefore, it is possible that impairment of the checkpoint response is involved in the process. In fact, the H2AX-diminished and growth-arrested state of primary WT MEFs is associated with an impaired checkpoint response [19]. In fact, canonical mitotic catastrophe-associated death was observed as a mechanism of cancer cell death after anti-cancer drug treatment [28–31]. Thus, primary WT MEFs that are protected from immortalization under diploidy but could escape from mitotic catastrophe with causing tetraploidization that is associated with mutation induction in Arf/p53 module. The resulting immortalized MEFs turn out sensitive to mitotic catastrophe-associated cell death due to mutation in Arf/p53 module.

Acknowledgments

This study was supported by a grant-in-aid for scientific research from the Ministry of Education, Culture, Sports, Science and Technology (20770136) and the National Cancer Center Research and Development Fund (23-C-10). We are grateful to N. Takamatsu and H. Nakagama for critical discussion of the study.

References

[1] S. Negrini, V.G. Gorgoulis, T.D. Halazonetis, Genomic instability—an evolving hallmark of cancer, Nature Reviews Molecular Cell Biology 11 (2010) 220–228.
[2] C. Lengauer, K.W. Kinzler, B. Vogelstein, Genetic instabilities in human cancers, Nature 396 (1998) 643–649.
[3] C. Lengauer, K.W. Kinzler, B. Vogelstein, Genetic instability in colorectal cancers, Nature 386 (1997) 623–627.